# TRIPLE-QUANTUM FILTERED CHLORINE MAGNETIC RESONANCE IMAGING OF THE HUMAN BRAIN

Alina Gilles[1], Nadia Benkhedah[1], Peter Bachert[1], Wolfhard Semmler[1], and Armin M. Nagel[1]
[1]*Dpt. of Medical Physics in Radiology, German Cancer Research Center (DKFZ), Heidelberg, Germany*

## Introduction

Chloride ($^{35}Cl^-$) is the most abundant anion in the mammalian organism and determines fundamental biological functions in all tissues. Its functions range from ion homeostasis to cell volume and intracellular pH regulation, transepithelial transport, and regulation of electrical excitability in nerve and muscle cells [1]. Chloride ions are actively transported and tightly regulated in virtually all cells of mammals. Alterations in the chloride homeostasis underlie various pathological conditions such as epilepsy, deafness, imbalance, brain edema, and neurogenic inflammation. Chloride ion channels and transporters expressed in the plasma membrane of primary brain tumor cells seem to play an important role in the migration of the tumor cells within the brain [2]. A higher intracellular chlorine concentration is thus associated with oncogenesis [3]. Also ischemic episodes in the CNS cause an increase of intracellular $^{35}Cl$ [4]. It is therefore highly desirable to develop imaging methods to obtain information about the intracellular $^{35}Cl$ level. However, there are no MRI studies of intracellular $^{35}Cl$ so far. Triple-quantum filtered (TQF) $^{35}Cl$ imaging might allow a weighting towards the intracellular $^{35}Cl$ content.
In this work, we present the first in vivo TQF $^{35}Cl$ images of the human brain and evaluate the feasibility for high field (7T) imaging.

## Methods

The TQF $^{35}Cl$ and, for comparative purposes, $^{23}Na$ imaging experiments were performed on a 7-T whole-body MR system (Magnetom 7 T, Siemens Healthcare, Erlangen, Germany) using two double resonant quadrature birdcage coils ($^{35}Cl/^{1}H$: QED, Mayfield Village, Ohio, USA; $^{23}Na/^{1}H$: Rapid Biomed GmbH, Rimpar, Germany).

**Phantom measurements** (Figs. 1, 2)
In order to optimize the TQF imaging sequence for in vivo measurements a phantom consisting of seven acrylic flasks (200 ml) was built. The flasks filled with sodium chloride (NaCl) solutions (153.9 mmol/l) containing different agar gel concentrations (1%, 2%, 3%, 4%, 5%, 6%, 7%) were attached inside a 4200-ml flask filled with pure NaCl solution. TQF $^{35}Cl$ and $^{23}Na$ images were first acquired from this phantom in order to determine transversal relaxation times $T_2$ precisely.
$T_2$ was measured using a standard three-pulse TQF sequence with six step phase cycling: $\pi/2 - \tau_1 - \pi/2 - \tau_2 - \pi/2 - TE -$ acq. ($\tau_2$ = 50 µs; TR = 300 ms; readout length $T_{RO}$ = 11 ms; projections = 4000; $T_A$ = 120 min; resolution: $(\Delta x)^3$ = (8 mm)$^3$; averages = 6). A series of TQF $^{35}Cl$ and $^{23}Na$ images was acquired by varying $\tau_1$ =TE in the range of 1 to 100 ms. The 3D-density adapted projection reconstruction [5] TQF data of signal intensity as a function of $\tau_1$ =TE was fitted by the biexponential function
$(\exp(-(t/T_{2l}))-\exp(-(t/T_{2s})))^2$ [6],
with a short ($T_{2s}$) and a long relaxation component ($T_{2l}$).

**Brain imaging** (Fig. 3)
3D-TQF $^{35}Cl$ images of the human brain (healthy volunteer, female, 25 years) were acquired using the standard TQF sequence. To estimate the optimal $\tau_1$ = TE in order to obtain maximum signal intensity, TQF signal of the brain was first acquired spectroscopically for different $\tau_1$ = TE. In accordance with phantom measurements of NaCl containing 5 % of agar gel TQF signal of $^{35}Cl$ was at maximum intensity for $\tau_1$ = TE = 2.5 ms.
Sequence parameters were set to $\tau_1$ = TE = 2.5 ms; TR = 160 ms; $\alpha = 90°$; $T_{RO}$ = 11 ms; 4000 projections; (15 mm)$^3$; Hamming filtering; $T_A$ = 64 min.
To compare triple-quantum filtered to unfiltered signal the second acquired average of the measurement was reconstructed additionally.

## Results

The performance of MR TQF $^{35}Cl$ imaging was tested on the phantom. The experiments showed that signal components of pure saline solution were completely suppressed in TQF $^{35}Cl$ images (Fig. 2). Transversal relaxation times $T_2$ for $^{35}Cl$ nuclei compared to $^{23}Na$ nuclei in different agar gel concentrations were determined. $T_2$ could be measured with high accuracy since TQF signal components decay only after initial increase so that TQF signal data enables a more precise measurement of $T_{2l}$ and $T_{2s}$. Tab. 1 shows the results of the biexponential curve fitting procedure for $T_2$. $^{35}Cl$ exhibits much shorter relaxation times than $^{23}Na$. The different values obtained for $T_{2l}$ in the range of 5 to 16 ms and $T_{2s}$ between 0.3 to 4 ms for $^{35}Cl$ are attributed to restricted molecular ion mobility.
TQF $^{35}Cl$ images of the human brain with SNR of 13 could be acquired with isotropic voxel size of (15 mm)$^3$ in 64 min (Fig. 3).

## Discussion and Conclusion

In this study we present the first in vivo TQF $^{35}Cl$ images. MRI of TQF $^{35}Cl$ suffers from low sensitivity due to low gyromagnetic ratio of $^{35}Cl$, fast relaxation and low intracellular concentration. However, for high fields ($B_0$ = 7 T) acquisition of TQF $^{35}Cl$ images is possible. Selective detection of $^{35}Cl$ nuclei which are exposed to quadrupolar interaction, i.e. intracellular $^{35}Cl$, is thus feasible. It has to be evaluated to what extent extracellular $^{35}Cl$ contributes to the TQF signal. Future monitoring of TQF $^{35}Cl$ signal may prove worthwhile in understanding the pathophysiological changes of ion concentration in various diseases including those of the central nervous system (e.g. ischemia and tumors).

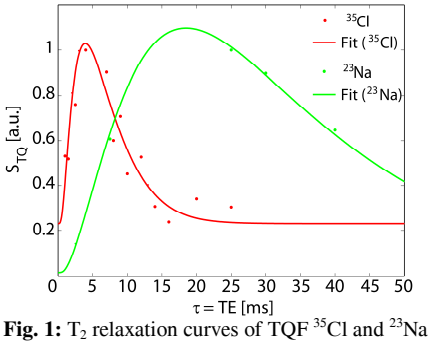


**Fig. 1:** $T_2$ relaxation curves of TQF $^{35}Cl$ and $^{23}Na$ signal of 153.9 mmol/l sodium chloride solution containing 2 % of agar gel.

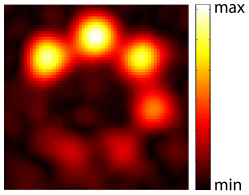


**Fig. 2**: TQF $^{35}Cl$ signal of NaCl flasks containing different concentrations of agar gel (clockwise 1-7 %). Signal of pure NaCl solution in the center of the phantom is suppressed.

**Tab. 1:** $^{35}Cl$ and $^{23}Na$ $T_2$ relaxation times of 153.9 mmol/l sodium chloride solution containing different concentrations of agar gel ($B_0$ = 7 T, T = 295 K).

| Agar | $^{35}Cl$ | | $^{23}Na$ | |
|---|---|---|---|---|
| [%] | $T_{2l}$ [ms] | $T_{2s}$ [ms] | $T_{2l}$ [ms] | $T_{2s}$ [ms] |
| 1 | 15.3 ± 5.3 | 3.1 ± 0.8 | 45,1 ± 3.6 | 16,6 ± 1.2 |
| 2 | 12.8 ± 3.2 | 1.7 ± 0.4 | 45,0 ± 16.2 | 9,3 ± 2.3 |
| 3 | 6.7 ± 1.5 | 1.1 ± 0.2 | 40,2 ± 14.4 | 7,9 ± 1.7 |
| 5 | 6.6 ± 1.7 | 0.5 ± 0.1 | 39,2 ± 7.1 | 4,9 ± 0.7 |
| 6 | 6.2 ± 2.3 | 0.3 ± 0.2 | 36,3 ± 3.7 | 3,5 ± 0.4 |
| 7 | 5.6 ± 2.9 | 0.3 ± 0.3 | 30,6 ± 2.2 | 3,2 ± 0.2 |

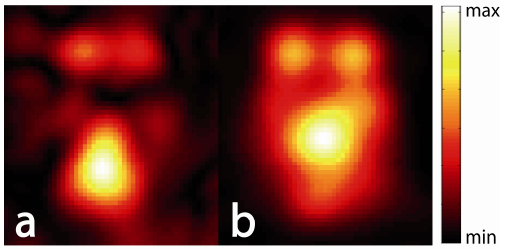


**Fig. 3:** Exemplary slices of triple quantum filtered (a) and unfiltered (b) $^{35}Cl$ signal in vivo of the human head (healthy volunteer). Signal of the eyes in the TQF image is partially suppressed.

## References

1. T. J. Jentsch *et al.*, J. Physiol. Rev. **82**, 503-568 (2002).
2. F. J. Alvarez-Leefmans and E. Delpire, *Physiology and Pathology of Chloride Transporters and Channels in the Nervous System* (Academic, San Diego, 2009).
3. I. L. Cameron *et al.*, Cancer Res. **40**, 1493-1500 (1980).
4. B. B. Pond *et al.*, J. Neurosci. **26** (5), 1396-1406 (2006).
5. A. M. Nagel *et al.*, Magn. Reson. Med. **62**, 1565-1573 (2009).
6. U. Eliav *et al.*, J. Magn. Reson. **128,** 82-86 (1997).